Electronic Supplementary Material (ESI) for Inorganic Chemistry Frontiers.

Electronic Supplementary Information

ZIF-8-Based *vs.* ZIF-8-Derived Au and Pd Nanoparticles as Efficient Nanocatalysts for the Ullmann Homocoupling Reaction

Wenjuan Wang,[a,b] Shuang Chen,[c] Eduardo Guisasola Cal,[d] Marta Martínez Moro,[d] Sergio Moya,[d] Emerson Coy, [e] Changlong Wang,[a] Jean-René Hamon,[b] and Didier Astruc[a,*]

[a.] *ISM, UMR CNRS 5255, Université de Bordeaux, Talence 33405 Cedex, France.* *E-mail: didier.astruc@u-bordeaux.fr*
[b.] *Institut des Sciences Chimiques, UMR CNRS 6226, Université de Rennes 1, 35042 Rennes Cedex, France.*
[c.] *Department of Chemistry and Center for Atomic Engineering of Advanced Materials, Anhui University, Hefei, Anhui 230601, China.*
[d.] *Soft Matter Nanotechnology Lab, CIC biomaGUNE, Paseo Miramón 182, 20014 Donostia-San Sebastián, Gipuzkoa, Spain.*
NanoBioMedical Centre, Adam Mickiewicz University in Poznań, Wszechnicy Piastowskiej 3, 61-614 Poznań, Poland

Table of contents

page

1. General data

All the solvents and chemicals were used as received. ^{1}H NMR spectra were recorded at 25 °C with a Bruker AC 300 MHz. All the chemical shifts are reported in parts per million (δ, ppm) with reference to Me_4Si in $CDCl_3$. X-ray diffraction (XRD) patterns were obtained on SmartLab 9KW with Cu Kα radiation. Nanoparticles loaded into the ZIF-8 were determined by Inductively Coupled Plasma Mass Spectrometry (ICP-MS). Transmission Electron Microscopy (TEM): The sizes of the MNPs were determined by TEM using a JEOL JEM 1400 (120 kV) microscope. The TEM samples were prepared by deposition of the nanoparticle suspension (10 μL) onto a carbon-coated microscopy copper grid. X-ray Photoelectron Spectroscopy (XPS): System: SPECS SAGE HR; X-Ray source: Al Kα non-monochromatic; operated at 12.5 kV and 300 W. Take off angle 90^o, at ~10^{-8} Torr. Pass energy for survey spectra 30 eV, 10 eV for narrow scans analysis; spectra are calibrated to CC carbon 285 eV. Analysis is consisted of Shirley background subtraction. Peaks are fitted with symmetrical Gaussian-Lorentizan (GL) line shapes. Samples are prepared by dehydration on the titania coated glass or silica substrates. Titania is selected as a substrate to avoid the overlap of Si and Au. Flash column chromatography was performed using silica gel (300-400 mesh).

2. Procedure for digestion of nanocatalysts with EDTA, and nanoparticles capping with PVP for TEM characterization.

A schlenk flask is charged with 20 mg of as-prepared Pd@ZIF-8 in 6 mL water, and this mixture is stirred continuously at room temperature. PVP (Mw=10000, 10 equiv per NPs) solubilized in 2 mL water is added and allowed to stir for 30 min. EDTA-2Na·$2H_2O$ (10 equiv) in 2 mL water is then added and the mixture is stirring for 1 h. Several drops of this solution are used for TEM characterization.

3. TEM and size distribution of ZIF-8, Au@CN and Pd@CN.

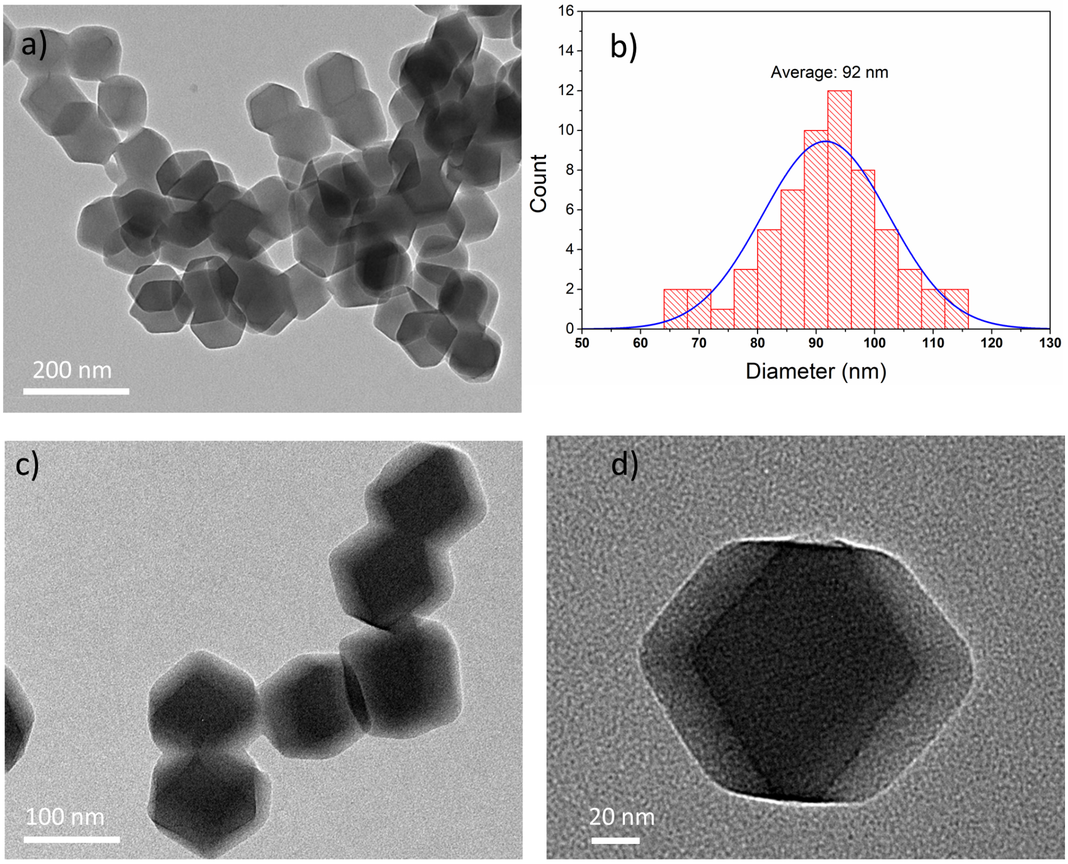

Fig. S1. TEM images and size distribution histogram of the ZIF-8.

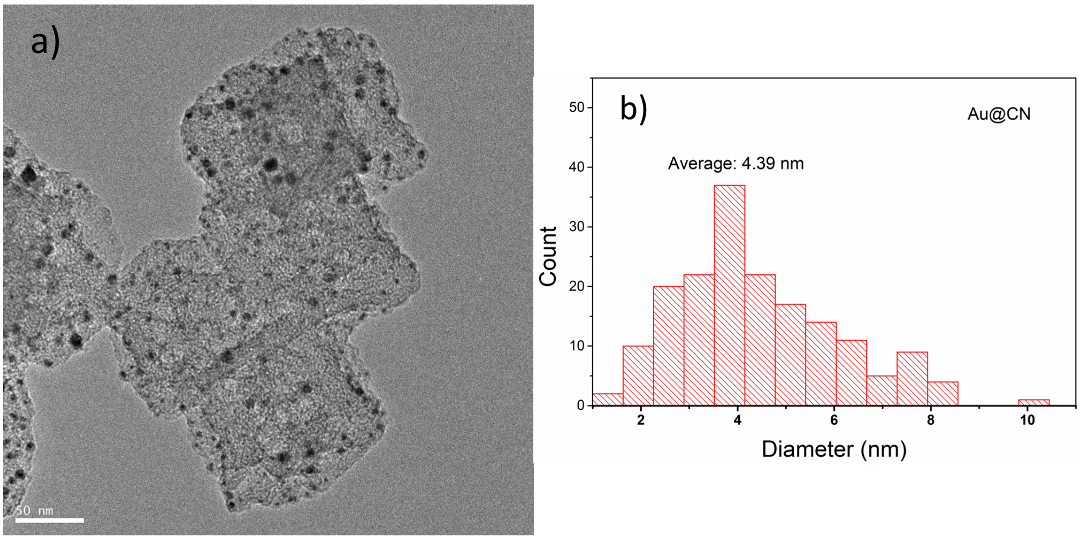

Fig. S2 TEM images and size distribution histogram of as-synthesized Au@CN.

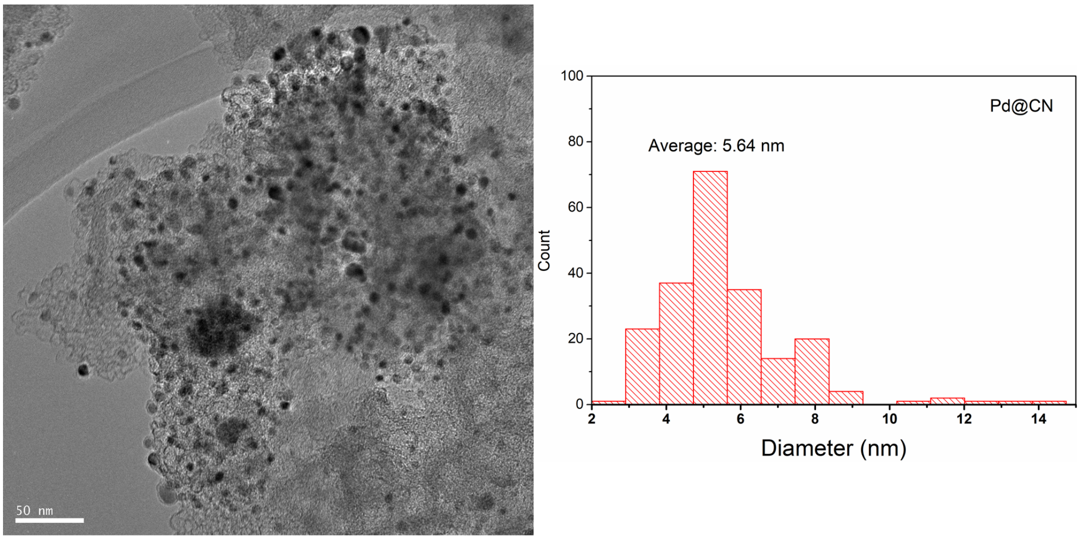

Fig. S3 TEM images and size distribution histogram of as-synthesized Pd@CN.

4. TEM and size distribution of Pd@ ZIF-8 and Au@ZIF-8 after reaction.

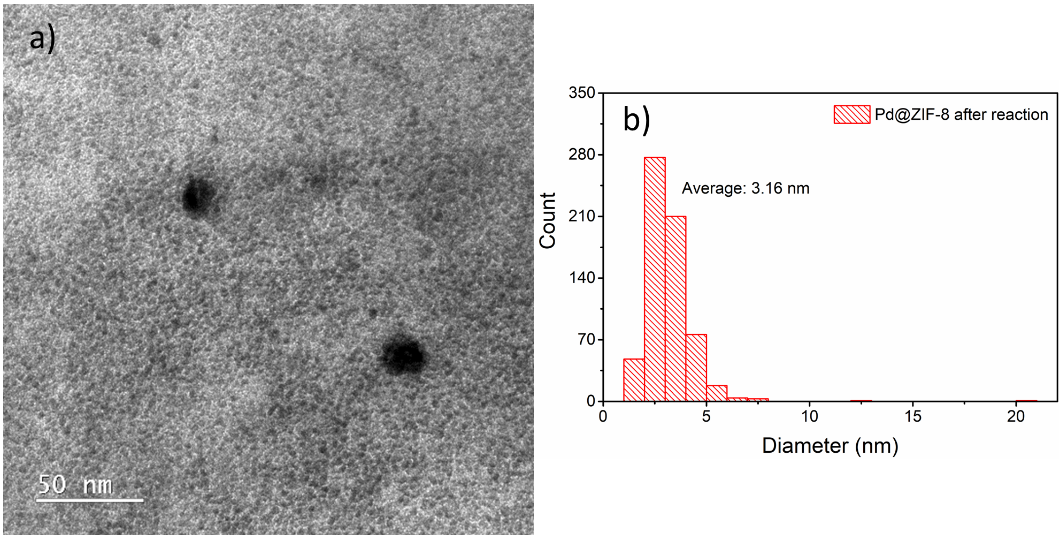

Fig. S4 TEM image (a) and size distribution (b) of Pd@ZIF-8 after reaction. Pd@ZIF-8 after digestion of the nanocatalyst with ethylenediamine tetracetic acid (EDTA) to release nanoparticles, and nanoparticles stabilized by PVP.

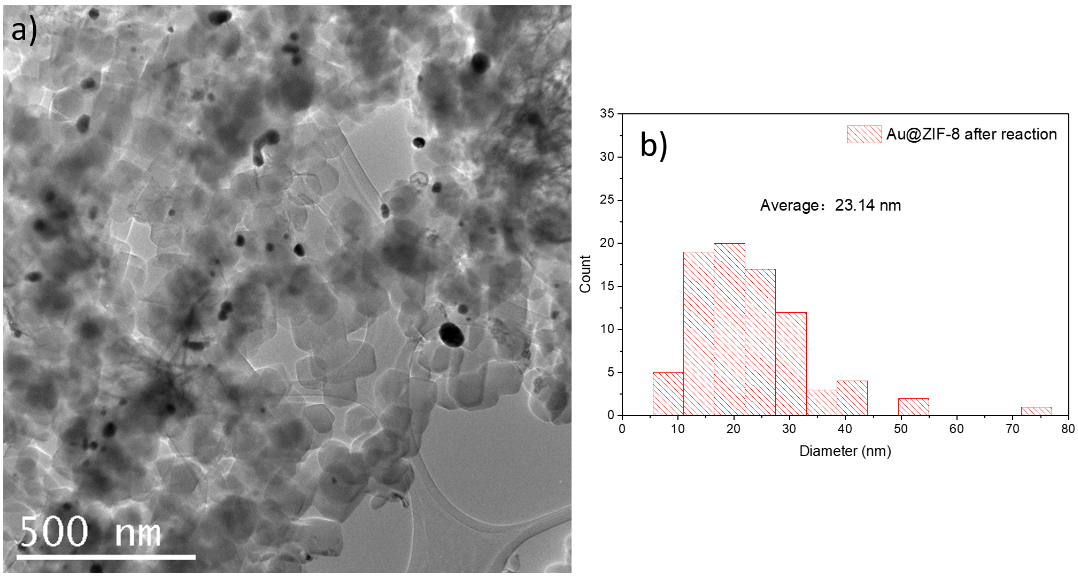

Fig. S5 TEM images and size distribution histogram of as-synthesized Au@ZIF-8 after reaction.

5. XRD patterns of ZIF-8, Pd@ZIF-8 and Au@ZIF-8

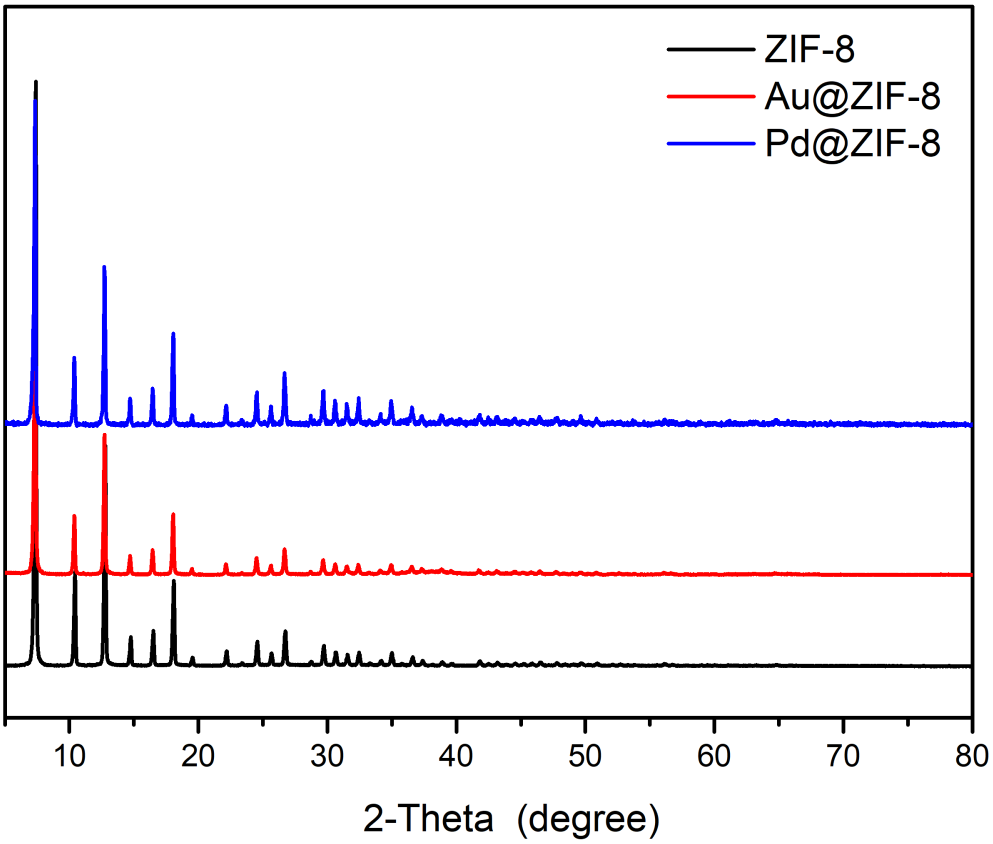

Fig. S6. XRD patterns of ZIF-8, Au@ZIF-8 and Pd@ZIF-8.

6. XPS spectrum of the Pd@ZIF-8 and Au@ZIF-8

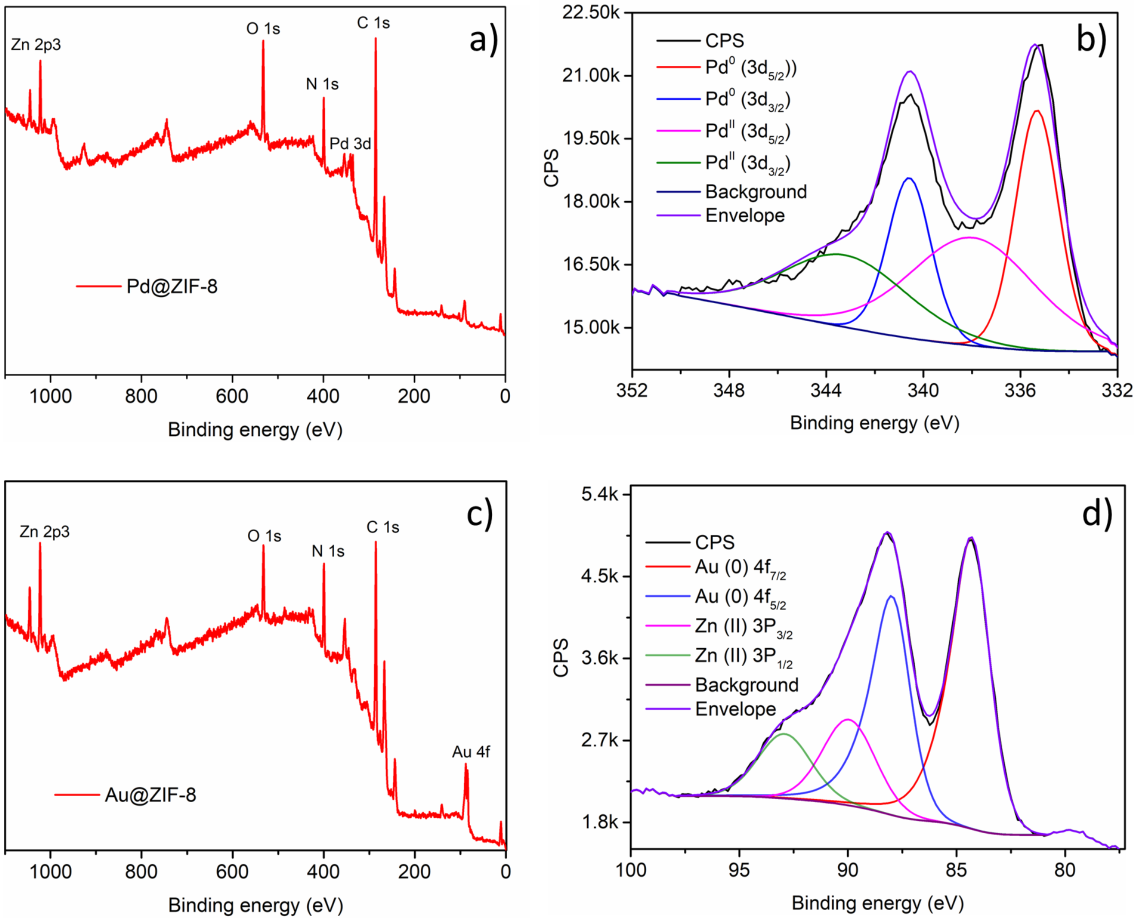

Fig. S7. XPS spectrum of the Pd@ZIF-8(a, b) and Au@ZIF-8 (c, d).

7. XPS spectrum of the Pd@ZIF-8 and Au@ZIF-8 after reaction

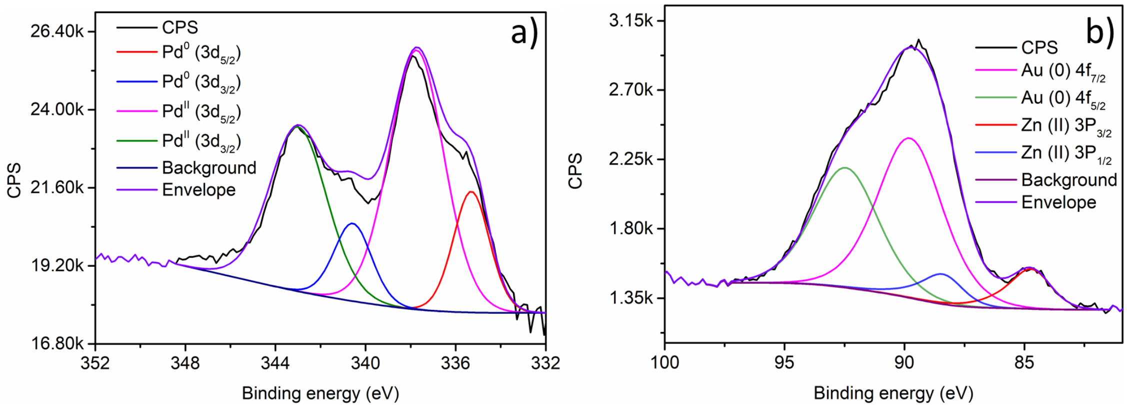

Fig. S8. XPS spectrum of the Pd@ZIF-8(a) and Au@ZIF-8 (b) after the catalytic reaction.

8. Physical properties of the nanocatalysts on ZIF-8, Au@ZIF-8 and Pd@ZIF-8

Table S1. Physical Properties of the Nanocatalysts on ZIF-8, Pd@ZIF-8 and Au@ZIF-8.

Sample	Surface area [$m^2.g^{-1}$]	Total Pore volume [$cm^3.g^{-1}$]	micropore volume [$cm^3.g^{-1}$]	Pore diameter [nm]
ZIF-8	1365.1	0.81	0.651	2.38
Au@ZIF-8	1283.1	0.85	0.595	2.64
Pd@ZIF-8	1247.7	0.66	0.581	2.07

9. Nanocatalysts for recycling experiments

Procedure for recycling the nanoparticle catalysts:

After the reaction, the system was allowed to cool to r.t.. The catalyst was washed with CH_2Cl_2, and with water by centrifugation respctively to remove iodobenzene and K_3PO_4, then dried at 60 °C under vacuum. After charging another run of substrates, DMF and K_3PO_4 , the system was purged with N_2 for 10 minutes. The reaction was then allowed to be proceeding. After 48 h, the reaction mixture was filtered. The liquid was extracted several times with CH_2Cl_2 and H_2O. The organic phase was dried over Na_2SO_4. Then CH_2Cl_2 was removed under reduced pressure at the rotary evaporator providing the crude product. ^1H NMR (300 MHZ, $CDCl_3$) was used to calculate the conversion.

Table S2. Effects of solvent, base and temperature on the homocoupling of iodobenzene catalyzed by Au@ZIF-8.

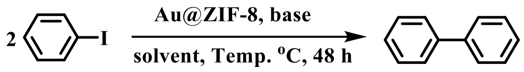

Entry	Solvent	Base	Temp. (°C)	Conversion (%) [a]
1	DMF	K_2CO_3	130	62
2	DMF	K_2CO_3	110	28
3	DMF	K_2CO_3	140	75
4	Xylene	K_2CO_3	140	11
5	PEG-400	K_2CO_3	140	74
6	DMF	K_3PO_4	140	83

Reaction conditions: 0.2 mmol iodobenzene, 0.6 mmol base, 1 mL solvent, 50 mg Au@ZIF-8 (6 mmol%), 140 °C, N_2, 48 h. a ^1H NMR conversion.

10. ^{1}H NMR spectra of various substrates with Pd@ZIF-8 as catalyst

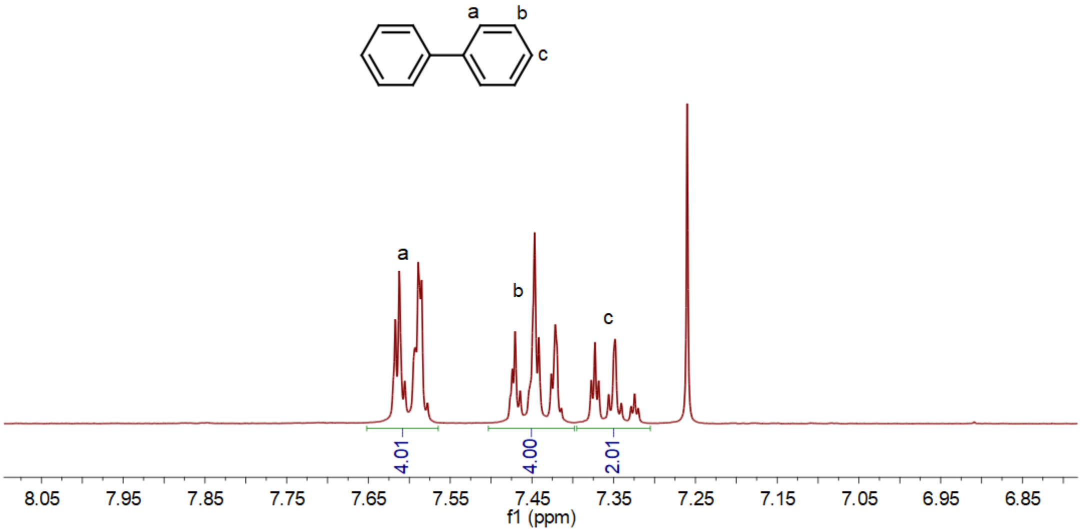

Fig. S9. ^{1}H NMR (300 MHZ, $CDCl_3$) spectrum of the product of 1,1'-biphenyl (homocoupling of iodobenzene with Pd@ZIF-8).

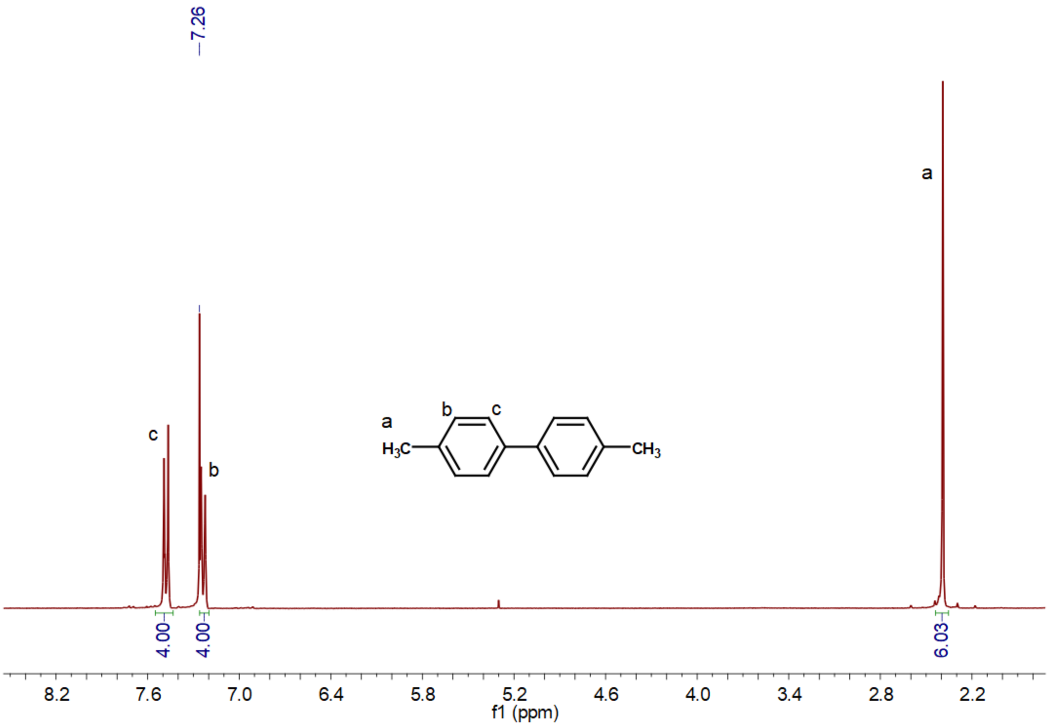

Fig. S10. ^{1}H NMR (300 MHZ, $CDCl_3$) spectrum of the product of 4,4'-dimethyl-1,1'-biphenyl (Homocoupling of iodotoluene with Pd@ZIF-8).

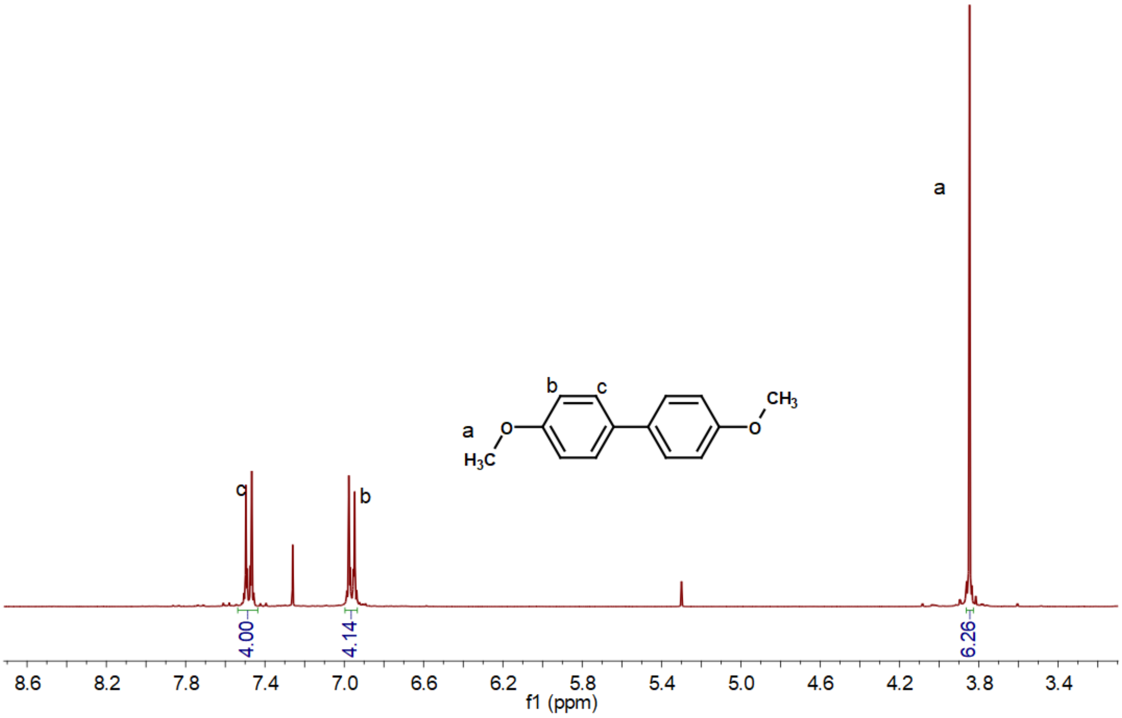

Fig. S11. ^{1}H NMR (300 MHZ, $CDCl_3$) spectrum of the product of 4,4'-dimethoxy-1,1'-biphenyl (homocoupling of iodoanisole with Pd@ZIF-8).

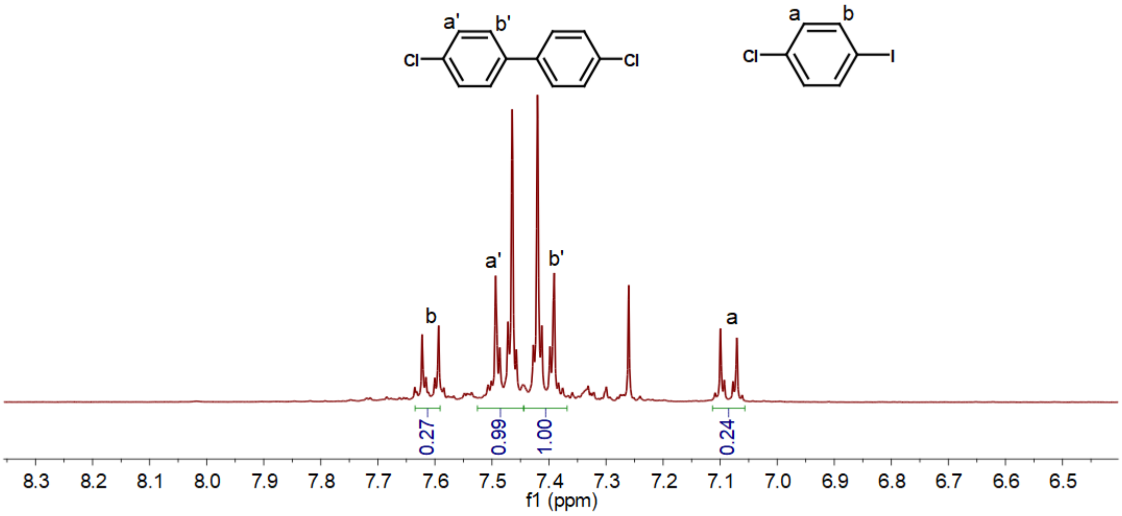

Fig. S12. ^{1}H NMR (300 MHZ, $CDCl_3$) spectrum of the crude product of 4,4'-dichloro-1,1'-biphenyl (Homocoupling of 1-chloro-4-iodobenzene with Pd@ZIF-8).

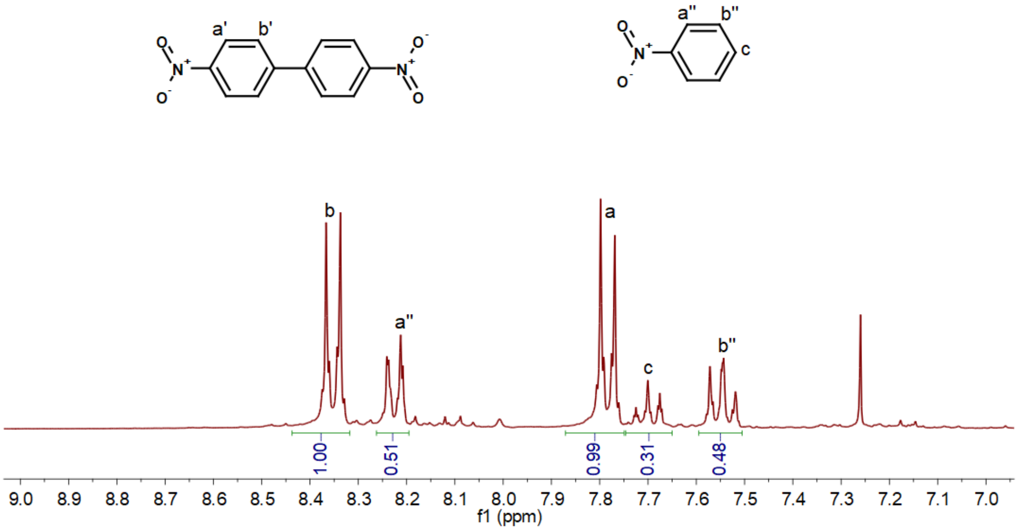

Fig. S13. ^{1}H NMR (300 MHZ, $CDCl_3$) Spectrum of the crude product of 4,4'-dinitro-1,1'-biphenyl (Homocoupling of 1-iodo-4-nitrobenzene with Pd@ZIF-8).

11. ^{1}H NMR spectra for various substrates with Au@ZIF-8 as catalyst

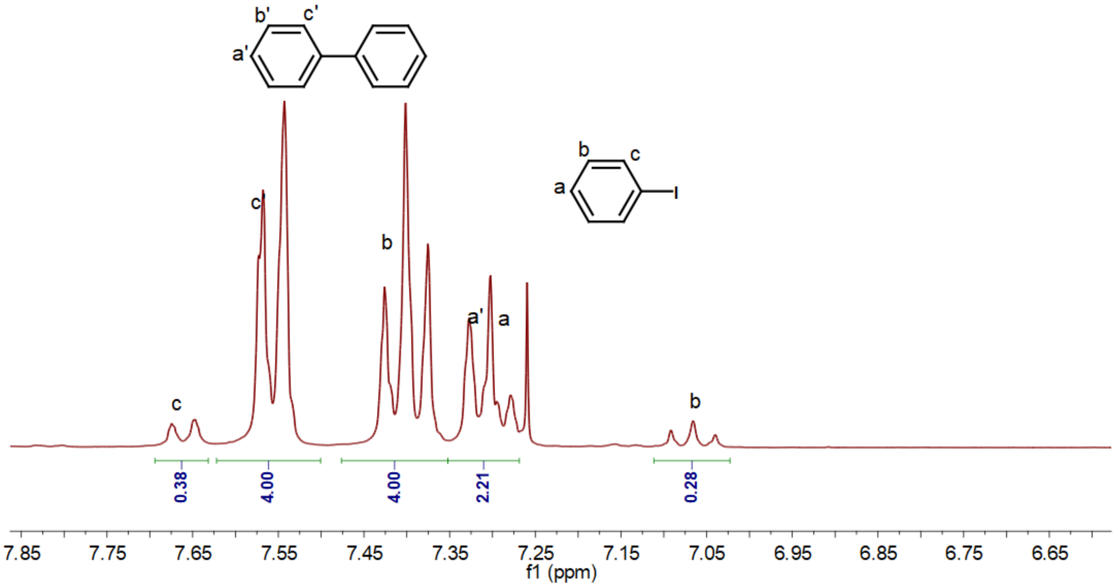

Fig. S14. ^{1}H NMR (300 MHZ, $CDCl_3$) Spectrum of the crude product of 1,1'-biphenyl (homocoupling of iodobenzene with Au@ZI-8).

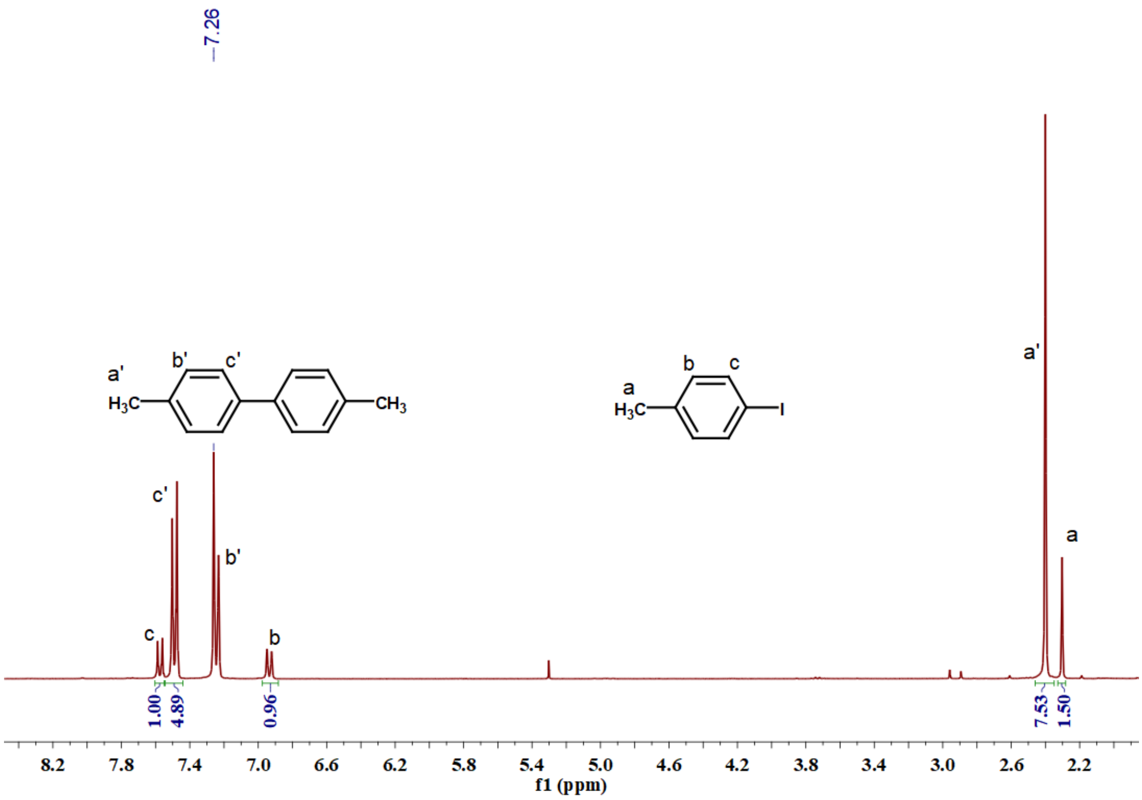

Fig. S15. ^{1}H NMR (300 MHZ, $CDCl_3$) Spectrum of the crude product of 4,4'-dimethyl-1,1'-biphenyl (Homocoupling of iodotoluene with Au@ZIF-8).

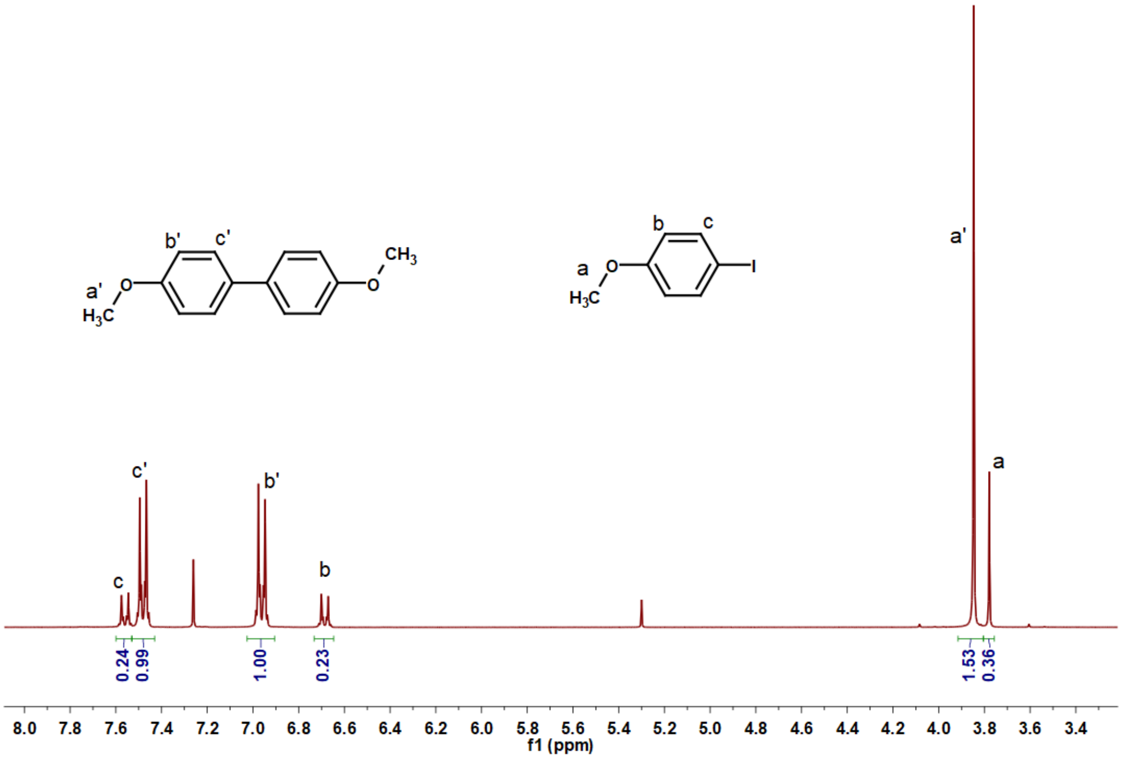

Fig. S16 ^{1}H NMR (300 MHZ, $CDCl_3$) Spectrum of the crude product of 4,4'-dimethoxy-1,1'-biphenyl (Homocoupling of iodoanisole with Au@ZIF-8).

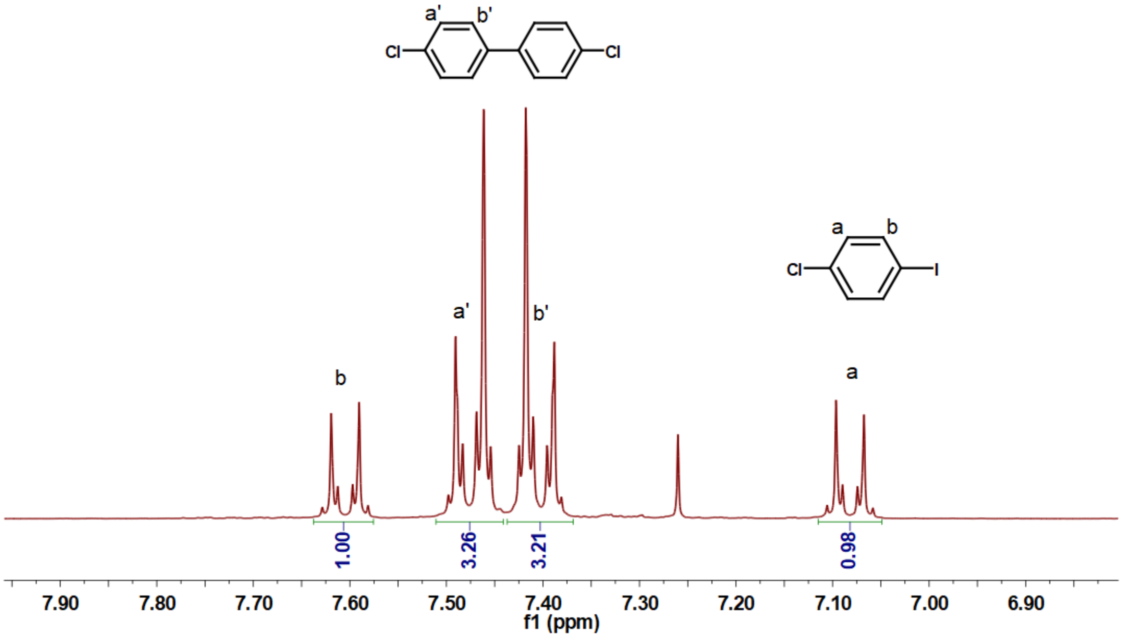

Fig. S17. ^{1}H NMR (300 MHZ, $CDCl_3$) spectrum of the crude product of 4,4'-dichloro-1,1'-biphenyl (Homocoupling of 1-chloro-4-iodobenzene with Au@ZIF-8).

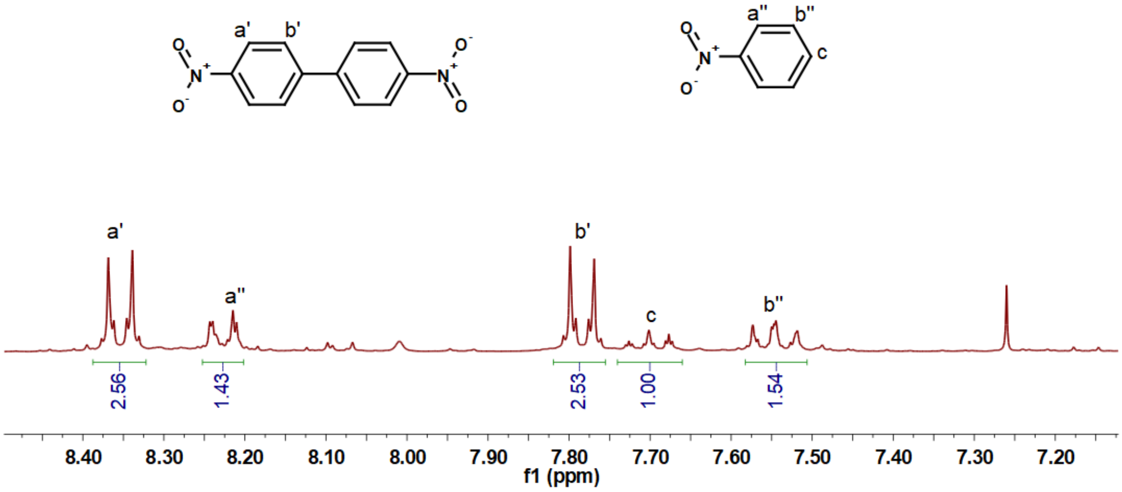

Fig. S18. ^{1}H NMR (300 MHZ, $CDCl_3$) spectrum of the crude product of 4,4'-dinitro-1,1'-biphenyl (Homocoupling of 1-iodo-4-nitrobenzene with Au@ZIF-8).